Performance of Maximum Ratio Transmission in Ad Hoc Networks With SWIPT

Xiaohui Zhou, *Student Member, IEEE*, Jing Guo, *Student Member, IEEE*, Salman Durrani, *Senior Member, IEEE*, and Ioannis Krikidis, *Senior Member, IEEE*

***Abstract*—This letter characterizes the performance of maximum ratio transmission (MRT) in ad hoc networks with simultaneous wireless information and power transfer (SWIPT). We assume that the transmitters are equipped with multiple antennas and use MRT, while the typical receiver is equipped with a single antenna and an energy harvesting receiver using time switching (TS) or power splitting (PS) receiver architectures. First, using stochastic geometry and considering the signal-to-interference plus noise ratio, we derive the exact outage probability at the reference receiver in closed-form. Simulation results confirm the accuracy of the derived analytical expressions. Then, we use the delay-tolerant throughput and delay-limited throughput, which are related to the outage probability, as metrics to study the system performance. The results show that for the delay-limited throughput, PS outperforms TS at low rate or at high energy harvesting ratio, respectively. For delay-tolerant throughput, PS always outperforms TS for any energy harvesting ratio.**

***Index Terms*—Throughput, maximum ratio transmission, simultaneous wireless information and power transfer, stochastic geometry.**

I. Introduction

SIMULTANEOUS wireless information and power transfer (SWIPT) is a promising solution to prolong the lifetime of nodes in 5G wireless systems [1]. The application of multiple antennas to SWIPT has recently been proposed as a means to improve the efficiency of radio frequency (RF) to direct current conversion, making implementing SWIPT really attractive for energy constrained wireless nodes [2]. Using stochastic geometry and *assuming single antenna nodes*, the performance of both traditional (i.e., non energy harvesting)[3], [4] and SWIPT enabled ad hoc networks [5], sensor networks [6] and cellular networks [7], [8] has been well studied in the literature.

Recently, some papers have used stochastic geometry to study the performance of traditional ad hoc networks [9]–[11] and cellular networks [12] with multiple antennas. The consideration of *multiple antennas* makes it extremely technically challenging to accurately analyze the interference. Prior work uses different approximations to characterize the interference in traditional multiple input multiple output (MIMO) ad hoc networks, e.g., a Taylor series expansion approximation is used in [9] and approximation using complicated special functions is used in [10]. The exact distribution of the signal-to-interference ratio (SIR) with maximum ratio combining (MRC) (i.e., multiple receive antennas) is derived in [11] for two receive antennas only. The exact distribution of the SIR with maximum ratio transmission (MRT) (i.e., multiple transmit antennas) is derived in [12] by a recursive approach using Toeplitz matrix form. Note that for tractability, majority of the prior work considers an interference limited network, i.e., SIR is used as the basis of the stochastic analysis [9], [11], [12]. The consideration of *multiple antennas with SWIPT* bring an additional challenge that the stochastic analysis must be based on signal-to-interference plus noise ratio (SINR), rather than SIR, in order to properly characterize SWIPT. To the best of our knowledge, the exact outage probability and throughput of MRT in ad hoc networks with integrated SWIPT (where information and power are extracted from the same RF signal) has not yet been derived in the literature.

Letter contributions: In this letter, we consider an ad hoc network consisting of multiple transmitters (TXs) which are modeled using a Poisson point process (PPP). The TXs are equipped with multiple antennas and use MRT. We consider the performance at a reference receiver (RX), which is equipped with a single antenna and energy harvesting receiver using time switching (TS) or power splitting (PS) receiver architectures. The novel contributions of this work are: (i) Employing stochastic geometry and considering the SINR, we derive the exact outage probability in closed-form for MRT in ad hoc networks with SWIPT (cf. Theorem 1). Simulation results confirm the accuracy of the derived expressions. (ii) Adopting the delay-limited and delay-tolerant throughput metrics [13], which are related to the outage probability, we study and compare the performance of TS and PS architectures. The results show that for the delay-limited throughput, where the TX transmits with a fixed rate, PS outperforms TS at low rate or at high energy harvesting ratio. For the delay-tolerant throughput, where the TX transmits at a rate equal to the ergodic capacity, PS outperforms TS for any energy harvesting ratio.

II. System Model

We consider a two-dimensional wireless ad hoc network region. The location of TXs is modeled as a homogeneous PPP with node density λ, denoted as Φ_t. In order to analyze the system performance, we add a reference receiver Y at the origin and its associated transmitter X_0 at a distance d_r in a random direction. Throughout the paper, we use X_i to denote both the random location as well as the i-th TX itself.

The wireless communication channel is modeled as a bounded path-loss plus block fading channel. The bounded path-loss between the i-th TX and the RX is [3], [5]

$$l(R_i) = \min\left\{r_0^{-\alpha}, R_i^{-\alpha}\right\}, \quad (1)$$

Manuscript received March 2, 2015; accepted June 26, 2015. Date of publication July 6, 2015; date of current version October 9, 2015. The associate editor coordinating the review of this paper and approving it for publication was K. Huang.

X. Zhou, J. Guo, and S. Durrani are with the Research School of Engineering, College of Engineering and Computer Science, Australian National University, Canberra, ACT 2601, Australia (e-mail: xiaohui.zhou@anu.edu.au; jing.guo@anu.edu.au; salman.durrani@anu.edu.au).

I. Krikidis is with the Department of Electrical and Computer Engineering, Faculty of Engineering, University of Cyprus, Nicosia 1678, Cyprus (e-mail: krikidis@ucy.ac.cy).

Digital Object Identifier 10.1109/LWC.2015.2452922

where $R_i = \|X_i - Y\|$ denotes the Euclidean distance between X_i and Y, α is the path-loss exponent and we define $\delta = \frac{2}{\alpha}$. r_0 is used in (1) to avoid the singularity at the origin. Note that we assume $d_r > r_0$ in this work. Moreover, all communication links experience the additive white Gaussian noise (AWGN) with variance σ^2.

Each TX is equipped with M antennas while the reference RX is equipped with a single omnidirectional antenna. Hence, the reference RX receives the desired signal as well as the interference from all transmissions. In this work, we consider MRT, where each TX sends a linearly weighted version of the same signal on each antenna [9]. As we consider a large-scale network region, we assume that each TX knows the channel state information (CSI) for its desired RX only. Then the signaling strategy becomes maximizing the signal-to-noise ratio over a specific channel [12]. Let $\mathbf{h}_i$ denote the fading between the i-th TX and its desired RX. Under MRT, the weighting vector is $\mathbf{a}_i = \frac{\mathbf{h}_i}{\|\mathbf{h}_i\|}$. We consider the Rayleigh fading scenario and hence $\mathbf{h}_i$ is a $M \times 1$ vector with independently and identically distributed (i.i.d.) unit variance and complex Gaussian entries, i.e., $\mathbf{h}_i \sim \mathcal{CN}(0, \mathbf{I}_M)$, where $\mathbf{I}_M$ is the identity matrix of size M.

The TXs have a dedicated power supply (e.g., battery or power grid) and transmit with constant power P_t. The reference RX has a battery to support its operation and uses RF energy harvesting to supplement its battery life. The energy harvesting is accomplished using either TS or PS receiver architecture [14]. In the TS receiver, each time block (T) is divided into two parts with TS ratio $\rho \in (0, 1)$: in $(1-\rho)T$ seconds the received power is used for rectification while in ρT seconds all the received power is used for data detection. In the PS receiver, the received power is divided into two parts with PS ratio $v_d \in (0, 1)$: $100(1 - v_d)\%$ of the received power is used for rectification while $100v_d\%$ of the received power is used for data detection. We further assume that the additional circuit noise introduced during the baseband conversion process in the RF energy harvesting circuit is modeled as AWGN with zero mean and variance σ_c^2 [5].

For the above setup, according to Slivnyaks Theorem [3], the instantaneous SINR at the reference RX can be expressed as

$$\text{SINR} = \begin{cases} \dfrac{P_t G_0 d_r^{-\alpha}}{P_t \sum\limits_{X_i \in \Phi_t} G_i l(R_i) + \sigma^2 + \sigma_c^2}, & \text{TS;} \\ \dfrac{v_d P_t G_0 d_r^{-\alpha}}{v_d \left(P_t \sum\limits_{X_i \in \Phi_t} G_i l(R_i) + \sigma^2 \right) + \sigma_c^2}, & \text{PS;} \end{cases} \triangleq \frac{P_r}{I_{\text{agg}} + \chi}, \quad (2)$$

where the fading power gain on the reference link is $G_0 = |\mathbf{h}_0^H \mathbf{a}_0|^2 = \|\mathbf{h}_0\|^2$, which follows the Gamma distribution with shape parameter M and scale parameter 1, the fading power gain between X_i and Y is $G_i = |\mathbf{h}_0^H \mathbf{a}_i|^2$, which is exponentially distributed [15], $|\cdot|$ is the magnitude operator, P_r is the received power at the reference RX from its desired TX, X_0, I_{agg} is the aggregate interference at the reference RX from other TXs and χ is $\sigma^2 + \sigma_c^2$ for TS and $\sigma^2 + \frac{\sigma_c^2}{v_d}$ for PS.

Throughput metrics: We adopt the throughput as the performance analysis metric, since it takes into account both the outage probability and the information decoding time T_{ID} ($T_{\text{ID}} = \rho T$ for TS receiver architecture and T for PS receiver architecture). In this letter, we consider both the delay-limited throughput and delay-tolerant throughput [13].

In the *delay-limited* transmission mode, the TX transmits with fixed rate R and information is successfully decoded if the SINR at the RX is greater than a threshold $\gamma_0 = 2^R - 1$. The throughput is evaluated over the effective information decoding time and is given by

$$\tau = \frac{T_{\text{ID}}}{T} \left(1 - p_{\text{out}}(2^R - 1, \chi)\right) R = \xi \left(1 - p_{\text{out}}(2^R - 1, \chi)\right) R. \quad (3)$$

In the *delay-tolerant* transmission mode, it is assumed that the code length is much larger than the block time so that the channel conditions average out and it is possible for the TX to have a transmission rate equal to the ergodic capacity $C \triangleq \mathbb{E}[\log_2(1 + \text{SINR})]$ [13]. Thus, the throughput is given by

$$\tau = \frac{T_{\text{ID}}}{T} C = \xi \int_0^\infty \left(1 - p_{\text{out}}(2^x - 1, \chi)\right) dx. \quad (4)$$

In both (3) and (4), ξ is ρ for TS and 1 for PS and $p_{\text{out}}(\cdot)$ is the outage probability, which is defined as the probability that the SINR at the typical RX is below a threshold γ_0 and is given by

$$p_{\text{out}}(\gamma_0, \chi) = \Pr(\text{SINR} < \gamma_0), \quad (5)$$

where $\Pr(\cdot)$ denotes the probability and SINR is given in (2).

III. Outage Probability Analysis

In this section, we provide the mathematical formulation and the main analytical result for outage probability at the reference RX, which then allows the throughput in (3) and (4) to be determined. Before we present the outage probability result, we define two lemmas.

Lemma 1: Given two functions $f(s)$ and $g(s)$, which are related as $f(s) = \exp(g(s))$, the h-th order derivative of $f(s)$, denoted as $f^{(h)}(s)$, can be expressed in terms of the h-th order derivative of $g(s)$, denoted as $g^{(h)}(s)$, as

$$f^{(h)}(s) = \sum \frac{h! \exp(g(s))}{p_1! p_2! \ldots p_h!} \left(\frac{g'(s)}{1!}\right)^{p_1} \left(\frac{g''(s)}{2!}\right)^{p_2} \cdots \left(\frac{g^{(h)}(s)}{h!}\right)^{p_h}, \quad (6)$$

where the sum is over all non-negative integer solutions of the Diophantine equation $p_1 + 2p_2 + \ldots + hp_h = h$.

Lemma 2: Define $a(s) \triangleq \exp(g_1(s))$ where $g_1(s) \triangleq \frac{-\pi\lambda r_0^{-\alpha+2} s}{1 + r_0^{-\alpha} s}$. Then the h-th order derivative of $a(s)$, $a^{(h)}(s)$, is obtained by substituting the h-th order derivative of $g_1(s)$ into (6), where $g_1^{(h)}(s)$ is given by

$$g_1^{(h)}(s) = \sum \frac{h! \pi \lambda r_0^{2-\alpha} (-1)^{q-1} q!}{q_1! q_2! \ldots q_h! \left(\frac{1}{s} + r_0^{-\alpha}\right)^{q+1}} \left(\frac{-1}{s^2}\right)^{q_1} \times \left(\frac{1}{s^3}\right)^{q_2} \cdots \left(\frac{(-1)^h}{s^{h+1}}\right)^{q_h}, \quad (7)$$

where the sum is over all non-negative integer solution of $q_1 + 2q_2 + \ldots + hq_h = h$ and $q = q_1 + q_2 + \ldots + q_h$.

Define $b(s) \triangleq \exp(g_2(s))$ where $g_2(s) \triangleq \frac{\pi\lambda s \, {}_2F_1(1, 1-\delta; 2-\delta; -r_0^{-\alpha} s)}{(1-1/\delta) r_0^{\alpha-2}}$. Then the h-th order derivative of $b(s)$, $b^{(h)}(s)$, is obtained by

substituting the h-th order derivative of $g_2(s)$ into (6), where $g_2^{(h)}(s)$ is given by

$$g_2^{(h)}(s) = \frac{{}_2F_1\left(1+h, 1-\delta+h; 2-\delta+h; -r_0^{-\alpha}s\right)}{(\delta-1)\left(-r_0^{\alpha}\right)^h\left(\pi\lambda r_0^{-\alpha+2}s\delta\right)^{-1}} \frac{1_{(h)}(1-\delta)_{(h)}}{(2-\delta)_{(h)}} + \binom{h}{1} \frac{{}_2F_1\left(h, h-\delta; 1-\delta+h; -r_0^{-\alpha}s\right)}{(\delta-1)\left(-r_0^{\alpha}\right)^{h-1}\left(\pi\lambda r_0^{-\alpha+2}\delta\right)^{-1}} \frac{1_{(h-1)}(1-\delta)_{(h-1)}}{(2-\delta)_{(h-1)}}, \tag{8}$$

where $x_{(n)} = \frac{(x+n-1)!}{(x-1)!}$ is the rising factorial and ${}_2F_1(\cdot,\cdot;\cdot;\cdot)$ is the Gaussian or ordinary hypergeometric function [16].

Proof: Lemma 1 and Lemma 2 can be proved using the chain rule [17] and simplifying. The details are omitted here due to space limitations. □

Using Lemmas 1 and 2, we can express the outage probability as shown in the following theorem.

Theorem 1: For an ad hoc network with SWIPT, where TXs perform maximum ratio transmission with M antennas and the reference RX has a single antenna, the outage probability at the reference RX is given by

$$p_{\text{out}}(\gamma_0, \chi) = 1 - \sum_{n=0}^{M-1} \frac{s^n}{n!}(-1)^n \exp\left(-s\frac{\chi}{P_t}\right) \sum_{k=0}^{n} \binom{n}{k} \times \left(\frac{-\chi}{P_t}\right)^{n-k} \sum_{h=0}^{k} \binom{k}{h} a^{(h)}(s) b^{(k-h)}(s), \tag{9}$$

where χ is defined below (2) , $s = \gamma_0 d_r^{\alpha}$, $a^{(h)}(s)$ and $b^{(k-h)}(s)$ are the higher-order derivatives of $a(s)$ and $b(s)$, which are presented in Lemma 2.

Proof: See Appendix A. □

Substituting Theorem 1 in (3) and (4), we can find the delay-limited throughput and the delay-tolerant throughput, respectively.

IV. Results

In this section, we present the analytical and simulation results. Unless otherwise stated, we set the parameters as follows: $d_r = 15$ m, $r_0 = 1$ m, $\lambda = 10^{-4}$, $P_t = 30$ dBm, $\sigma^2 = -130$ dBm, $\sigma_c^2 = -30$ dBm and $\alpha = 4$ [1]. The simulation results are obtained by averaging over 1 million Monte carlo realizations.

Delay-limited throughput: Fig. 1 plots the delay-limited throughput versus the transmission rate, R, using PS and TS receiver architectures ($\rho = v_d = 0.5$), with different number of antennas $M = 1, 2, 4, 8$. We can see that the simulation results match perfectly with the analytical results, which is to be expected since the analytical results are exact. The figure also shows that when the rate is small, PS outperforms TS and vice versa at high rate. This can be intuitively explained as follows. According to (3), the throughput is determined by both outage probability $p_{\text{out}}(\cdot)$ and information decoding time T_{ID}. The rate directly impacts $p_{\text{out}}(\cdot)$ but not T_{ID}. Thus, for small value of the rate (equivalently small γ_0), the outage probability difference between TS and PS receiver architectures is small. However, the effective information decoding time is only ρT for TS compared to the whole time block T for PS. Thus PS outperforms TS. When the rate is large, the outage probability difference between TS and PS becomes large. Thus, $p_{\text{out}}(\cdot)$ plays the dominant role in determining the throughput and TS outperforms PS. This interplay of $p_{\text{out}}(\cdot)$ and T_{ID} leads to the above mentioned throughput trends.

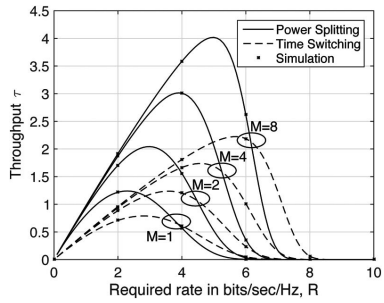

Fig. 1. Delay-limited throughput, τ, versus rate, R, for TS and PS receiver architectures.

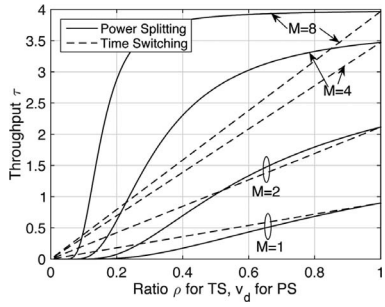

Fig. 2. Delay-limited throughput, τ, versus ratio (ρ for TS and v_d for PS).

Fig. 2 plots the delay-limited throughput versus the energy harvesting ratio (ρ for TS and v_d for PS), with different number of antennas $M = 1, 2, 4, 8$ and rate $R = 4.5$ bits/sec/Hz. The figure shows that increasing the energy harvesting ratio improves the throughput for both PS and TS receiver architectures. This is because increasing ρ increases T_{ID} for TS and increasing v_d decreases $p_{\text{out}}(\cdot)$ for PS, both of which lead to higher throughput. The figure also shows that when the energy harvesting ratio (ρ for TS and v_d for PS) is large, PS outperforms TS and vice versa for low energy harvesting ratio. This can be intuitively explained using similar arguments as before. For the given rate R, when the energy harvesting ratio is small, the aggregate noise χ for PS is much greater than that for TS, causing the $p_{\text{out}}(\cdot)$ for TS to be much smaller than that for PS. Thus, TS outperforms PS. When the energy harvesting ratio is large, $p_{\text{out}}(\cdot)$ becomes quite similar for both TS and PS and T_{ID} (or ξ) governs the throughput performance. Thus, PS outperforms TS in this case. Furthermore, it can also be observed from Fig. 2 that the throughput performance gain by increasing the number of TX antennas is more significant for PS, compared to TS.

Delay-tolerant throughput: Fig. 3 plots the delay-tolerant throughput versus the energy harvesting ratio (ρ for TS and v_d for PS), with different number of antennas $M = 1, 2, 4, 8$. We can see that the simulation results match perfectly with the analytical results. Fig. 3 shows that PS always outperforms TS. This trend is due to the fact that for the delay-tolerant throughput, the information decoding time T_{ID} (or ξ) plays the dominant role in determining the throughput performance. Comparing Fig. 3 with Fig. 2, we can see that for both receiver architectures, the achievable throughput in the delay-tolerant mode is always higher than in the delay-limited mode. This particular trend is due to the difference in the definition of the two modes and has also been observed in [13] for a relay-based energy harvesting network.

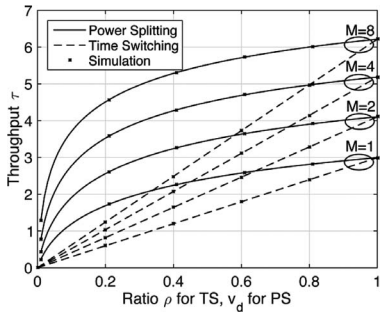

Fig. 3. Delay-tolerant throughput, τ, versus ratio (ρ for TS and v_d for PS).

V. Conclusion

In this letter, we have analyzed the performance of MRT in ad hoc networks with SWIPT. Using the SINR, we have derived the exact closed-form expression for the outage probability considering both TS and PS receiver architectures. Adopting the delay-limited and delay-tolerant throughput, which are related to the outage probability, we have analyzed the impact of the important system parameters (such as number of transmit antennas and energy harvesting ratio) on the throughput performance. The results showed that for the delay-limited throughput PS outperforms TS at low rate or at high energy harvesting ratio, while for the delay-tolerant throughput PS outperforms TS for any energy harvesting ratio. Future work can consider interesting extensions such as MIMO ad hoc networks with SWIPT, effect of imperfect CSI and power allocation between the two phases for TS receiver architecture.

Appendix A
Proof of Theorem 1

We derive a closed-form expression for outage probability using stochastic geometry and the reference-link-power-gain based (RLPG-based) framework [4]. The basic principle of this approach is to first condition on the interference and formulate the outage probability in terms of the cumulative distribution function of the reference link's fading power gain. The conditioning on the interference is then removed by first unconditioning on the fading power gains of the interference links and then unconditioning on the locations of the interferers.

Since the fading gain on reference link is Gamma distributed, we can rewrite the outage probability in (5) as

$$\begin{aligned} p_{\text{out}} &= \Pr\left(G_0 < \gamma_0 d_r^{\alpha}\frac{I_{\text{agg}}}{P_t} + \frac{\gamma_0\chi}{P_t d_r^{-\alpha}}\right) \\ &= 1-\mathbb{E}\left[\sum_{n=0}^{M-1}\frac{1}{n!}\left(s\left(I'_{\text{agg}}+\frac{\chi}{P_t}\right)\right)^n \exp\left(-s\left(I'_{\text{agg}}+\frac{\chi}{P_t}\right)\right)\right] \\ &= 1-\sum_{n=0}^{M-1}\frac{(-s)^n}{n!}\frac{d^n}{ds^n}\left(\mathcal{L}_{I'_{\text{agg}}}(s)\exp\left(\frac{-s\chi}{P_t}\right)\right) \\ &= 1-\sum_{n=0}^{M-1}\frac{(-s)^n}{n!}\exp\left(\frac{-s\chi}{P_t}\right)\sum_{k=0}^{n}\binom{n}{k}\left(\frac{-\chi}{P_t}\right)^{n-k}\frac{d^k}{ds^k}\mathcal{L}_{I'_{\text{agg}}}(s), \end{aligned} \tag{10}$$

where $I'_{\text{agg}} = \sum_{X_i\in\Phi_t} G_i l(R_i)$ and $s \triangleq \gamma_0 d_r^{\alpha}$. Note that $\mathcal{L}_{I'_{\text{agg}}}(s) = \mathbb{E}\left[\exp\left(-sI'_{\text{agg}}\right)\right]$ and it is the Laplace transform of I'_{agg}. Using stochastic geometry and the definition of Laplace transform, we then have

$$\begin{aligned} \mathcal{L}_{I'_{\text{agg}}}(s) &= \mathbb{E}_{\Phi_t}\left[\prod_{i\in\Phi_t, R_i\le r_0}\mathbb{E}_{G_i}\left[\exp\left(-sr_0^{-\alpha}G_i\right)\right]\right] \\ &\quad\times\mathbb{E}_{\Phi_t}\left[\prod_{i\in\Phi_t, R_i> r_0}\mathbb{E}_{G_i}\left[\exp\left(-sR_i^{-\alpha}G_i\right)\right]\right] \\ &= \exp\left(-\pi\lambda r_0^2\frac{sr_0^{-\alpha}}{sr_0^{-\alpha}+1}\right) \\ &\quad\times\exp\left(\pi\lambda r_0^2\frac{sr_0^{-\alpha}}{sr_0^{-\alpha}+1}+g_1(s)+g_2(s)\right) \\ &= \exp\left(g_1(s)+g_2(s)\right), \end{aligned} \tag{11}$$

where $g_1(s) = \frac{-\pi\lambda r_0^{-\alpha+2}s}{1+r_0^{-\alpha}s}$, $g_2(s) = \frac{\pi\lambda s_2 F_1(1,1-\delta;2-\delta;-r_0^{-\alpha}s)}{(1-1/\delta)r_0^{\alpha-2}}$.

Substituting (11) in (10), the calculation of outage requires the higher order derivatives of $\mathcal{L}_{I'_{\text{agg}}}(s)$, which have been presented in Lemma 1 and Lemma 2. Using Lemma 1 and 2, we arrive at the result in Theorem 1.

References

[1] X. Lu, P. Wang, D. Niyato, D. I. Kim, and Z. Han, "Wireless networks with RF energy harvesting: A contemporary survey," *IEEE Commun. Surveys Tuts.*, vol. 17, no. 2, pp. 757–789, 2nd Quart. 2015.

[2] Z. Ding *et al.*, "Application of smart antenna technologies in simultaneous wireless information and power transfer," *IEEE Commun. Mag.*, vol. 53, no. 4, pp. 86–93, Apr. 2015.

[3] M. Haenggi, *Stochastic Geometry for Wireless Networks*. Cambridge, U.K.: Cambridge Univ. Press, 2013.

[4] J. Guo, S. Durrani, and X. Zhou, "Outage probability in arbitrarily-shaped finite wireless networks," *IEEE Trans. Commun.*, vol. 62, no. 2, pp. 699–712, Feb. 2014.

[5] I. Krikidis, "Simultaneous information and energy transfer in large-scale networks with/without relaying," *IEEE Trans. Commun.*, vol. 62, no. 3, pp. 900–912, Mar. 2014.

[6] I. Flint, X. Lu, N. Privault, D. Niyato, and P. Wang, "Performance analysis of ambient RF energy harvesting with repulsive point process modelling," *IEEE Trans. Wireless Commun.*, to be published. [Online]. Available: http://ieeexplore.ieee.org/xpl/articleDetails.jsp?arnumber=7113917

[7] K. Huang, M. Kountouris, and V. O. K. Li, "Renewable powered cellular networks: Energy field modeling and network coverage," *IEEE Trans. Wireless Commun.*, vol. 14, no. 8, pp. 4234–4247, Aug. 2015.

[8] K. Huang and V. K. N. Lau, "Enabling wireless power transfer in cellular networks: Architecture, modeling and deployment," *IEEE Trans. Wireless Commun.*, vol. 13, no. 2, pp. 902–912, Feb. 2014.

[9] A. M. Hunter, J. G. Andrews, and S. Weber, "Transmission capacity of ad hoc networks with spatial diversity," *IEEE Trans. Wireless Commun.*, vol. 7, no. 12, pp. 5058–5071, Dec. 2008.

[10] Y. Wu, R. H. Y. Louie, M. R. McKay, and I. B. Collings, "Generalized framework for the analysis of linear MIMO transmission schemes in decentralized wireless Ad Hoc networks," *IEEE Trans. Wireless Commun.*, vol. 11, no. 8, pp. 2815–2827, Aug. 2012.

[11] R. Tanbourgi, H. S. Dhillon, J. G. Andrews, and F. K. Jondral, "Effect of spatial interference correlation on the performance of maximum ratio combining," *IEEE Trans. Wireless Commun.*, vol. 13, no. 6, pp. 3307–3316, Jun. 2014.

[12] C. Li, J. Zhang, and K. B. Letaief, "Throughput and energy efficiency analysis of small cell networks with multi-antenna base stations," *IEEE Trans. Wireless Commun.*, vol. 13, no. 5, pp. 2505–2517, May 2014.

[13] A. Nasir, X. Zhou, S. Durrani, and R. Kennedy, "Relaying protocols for wireless energy harvesting and information processing," *IEEE Trans. Wireless Commun.*, vol. 12, no. 7, pp. 3622–3636, Jul. 2013.

[14] R. Zhang and C. K. Ho, "MIMO broadcasting for simultaneous wireless information and power transfer," *IEEE Trans. Wireless Commun.*, vol. 12, no. 5, pp. 1989–2001, May 2013.

[15] A. Shah and A. M. Haimovich, "Performance analysis of maximal ratio combining and comparison with optimum combining for mobile radio communications with cochannel interference," *IEEE Trans. Veh. Technol.*, vol. 49, no. 4, pp. 1454–1463, Jul. 2000.

[16] I. S. Gradshteyn and I. M. Ryzhik, *Table of Integrals, Series, and Products*, 7th ed. New York, NY, USA: Academic, 2007.

[17] H. Huang, S. Marcantognini, and N. Young, "Chain rules for higher derivatives," *Math. Intell.*, no. 28, pp. 61–69, 2005.